RDR 2025-008

Research Data & Reports

Volume 1, Issue 1 (2025)
Journal homepage: https://researchdr.in

Investigating salt weathering performance of TEOS-consolidated brick masonry with naturally carbonated lime mortar

V.A. Anupama[1*], Enrico Sassoni[2] and Manu Santhanam[3]

[1]Doctoral research scholar, Department of Civil Engineering, Indian Institute of Technology Madras, Chennai, India, Email: vaanupama9@gmail.com
[2]Associate Professor, Department of Civil, Chemical, Environmental, and Materials Engineering, University of Bologna, Italy, Email: enrico.sassoni2@unibo.it
[3]Professor, Department of Civil Engineering, Indian Institute of Technology Madras, Chennai, India, Email: manusanthanam@gmail.com
* Corresponding author

A B S T R A C T

Consolidants are used widely in stone sculptures, statues and building units to improve the cohesion between the grains, increase mechanical strength and thereby improve the material durability. Although they are widely used in conservation projects, their performance in brick masonry, especially under salt weathering conditions, demands further research. This study aims to study the behaviour of brick-lime mortar masonry systems under accelerated salt weathering after consolidation with tetraethoxysilane (TEOS). Mass loss monitoring, mineralogical characterisation and microstructural analysis were performed to evaluate the alterations in the substrates, which are influenced by the salt type, crystallisation mechanism, consolidant composition and substrate mineralogy. The weathered brick-mortar sandwiches were sheared to understand the role played by consolidants on the mechanical performance of the composite system. The results indicate that while TEOS improved the mechanical performance of bricks and mortars, both individually and as composite systems, the accompanying pore structure modifications may increase crystallisation pressures and restrict moisture transport, with possible implications for long-term durability.

Keywords: *Consolidation, Salt weathering, Tetraethoxysilane, Masonry*

1 Introduction

Masonry structures in coastal and salt-laden environments are particularly vulnerable to deterioration driven by coupled hygrothermal fluctuations, moisture transport, and salt ingress. Among these factors, salt weathering is one of the most destructive mechanisms affecting porous building materials, as repeated dissolution and crystallisation cycles progressively alter pore networks, reduce grain cohesion, and ultimately lead to surface loss and mechanical weakening [1]. Salt weathering severely damages porous building materials by altering their microstructure and reducing their integrity. Dissolved salts from moisture sources crystallise during drying, generating stresses that crack and interconnect pores, accelerating deterioration [2]. The severity of this deterioration is influenced by the type of salt, the substrate's mineral composition and pore characteristics, and environmental conditions [3]. Given the complex interacting factors, enhancing the material's inherent resistance through consolidation becomes essential for long-term preservation. In conservation practice, surface consolidation is widely employed to counteract such degradation by restoring near-surface cohesion and mechanical strength [4], [5], [6], [7], [8].

Consolidants penetrate the porous fabric and form binding phases that strengthen deteriorated materials; however, their effectiveness is intrinsically linked to compatibility with the substrate. Advances in conservation highlight tetraethoxysilane (TEOS), which hydrolyses and polymerises within pores to form silica gel that strengthens the material, though it may also occlude pores and hinder moisture transport, which could significantly impact the weathering response of masonry systems [9]. The presence of salt can undermine the bond between substrate and consolidant and may lead to further deterioration in heterogeneous materials like brick–mortar composites, as consolidants can either mobilise the salt or trap it within cracks [10], [11]. These concerns are amplified in heterogeneous masonry assemblies, such as brick-mortar systems, where differences in pore structure and hygric behaviour between components can lead to preferential salt transport, interfacial stress concentration, and uneven degradation. Despite extensive application of TEOS in conservation practice, its performance under salt weathering conditions, particularly at the system scale and in the presence of aggressive salts such as sodium sulphate, remains insufficiently understood. The salt weathering performance of consolidated masonry could vary depending on the consolidant and substrate factors. While the effects of different salts have been explored in bricks [12], [13], stones [6], [13], [14] and mortars [15], [16], comparable investigations are still lacking for mineralogically and mechanically heterogeneous systems such as brick-mortar assemblies.

Against this background, the present study investigates the performance of TEOS consolidation in brick masonry subjected to

https://doi.org/ 10.70002/iitm.rdr.1.1.49
Received on 28 December 2025, Accepted on 22 January 2026, Available online 25 February 2026
Publisher: Centre of Excellence (CoE) on Technologies for Low Carbon and Lean Construction (TLC2) at Indian Institute of Technology Madras

chloride and sulphate weathering. By examining bricks, mortars, and brick–mortar composite specimens, the study aims to elucidate how TEOS-induced microstructural changes influence salt ingress, crystallisation behaviour, and mechanical response. Accelerated weathering cycles in NaCl and Na_2SO_4 solutions were combined with gravimetric analysis, mineralogical characterisation (XRD), microstructural investigation (SEM-EDS, MIP), and mechanical testing. The results provide insight into the balance between beneficial consolidation effects and potential salt-related risks, contributing to a more informed and performance-based assessment of consolidation strategies for masonry exposed to saline environments.

2 Materials and methods

2.1 Raw materials

The study used Class 5 fired clay bricks, hydrated lime, distilled water, and standard sands (zones I–III) to cast specimens. Sodium chloride and anhydrous sodium sulphate served as weathering agents. After initial laboratory salt exposure, specimens were desalinated via cellulose poulticing and consolidated with TEOS. Both consolidated and control specimens were then subjected to salt weathering to assess the impact of consolidation on resistance to salt attack.

2.2 Weathering specimen preparation

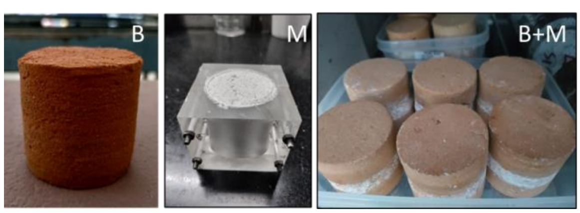

Figure 1 Specimens used for the study

Cylindrical specimens (50 ± 0.5 mm height and diameter) were used for weathering studies. Bricks were core-drilled from brick samples, while lime mortar was cast in acrylic molds (Figure 1) with a water-to-binder ratio of 0.85, achieving 165 mm flow and 89% water retention. Mortar specimens were demoulded after 7 days and exposed to natural carbonation for 28 days (labelled as "Mortar"). Sandwich specimens, with a 10 mm mortar layer between 20 mm brick slices, were also exposed to natural carbonation for 28 days (labelled as "B+M").

2.3 Weathering, consolidation and characterisation

Accelerated salt weathering followed the RILEM TC 271-ASC protocol using 10 wt% NaCl and 5 wt% Na_2SO_4 solutions introduced by capillary absorption [17]. Specimens were re-wetted with the same solutions during propagation, unlike with distilled water as per the recommended procedure, desalinated after two cycles, consolidated, and subjected to six additional chloride and seven sulphate weathering cycles.

TEOS consolidation was carried out using Estel 1000 (C.T.S. s.r.l., Italy; viscosity ≈10 mPa•s), applied by brushing (50 strokes) on the lateral surface of the desalinated specimens and cured at 22 ± 2 °C for 28 days. To enhance mechanical performance and reduce hydrophobicity, specimens were subsequently poulticed (1:4 poultice-to-water ratio) following the desalination procedure and oven-dried at 40 °C for three days [14]. Procedure for TEOS consolidation is illustrated in Figure 2.

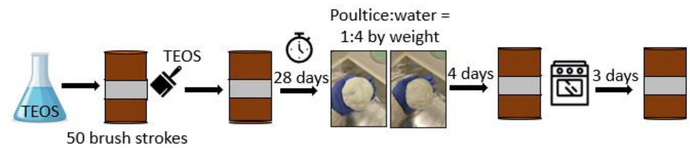

Figure 2 Procedure for TEOS consolidation

Mercury Intrusion Porosimetry (MIP) was employed to assess post-weathering changes in the material's porosity and pore size distribution. Brick-mortar interfaces in the composite specimens were examined using an Apreo-S field-emission SEM. Backscattered electron imaging combined with EDAX elemental mapping was employed to characterise salt distribution and localisation at the interface and within the specimen matrix. Weathered specimen phases were identified by XRD (MiniFlex Rigaku, CuKα, λ = 1.5405 Å, 45 kV, 15 mA). Samples from the bottom, mid-depth, and top surfaces were analysed over 5°-70° (2θ) at 10° min^{-1} with a 0.01° step. The shear strength of the composite systems was tested using a fabricated setup in the ZWICK tensile strength testing machine, applying a tensile force through the top clamp while the bottom clamp remained fixed.

A summary of the weathering and consolidation conditions is reported in Table 1.

Table 1 Sample labelling system

	Brick		Mortar		Brick+Mortar sandwich	
	NaCl	Na_2SO_4	NaCl	Na_2SO_4	NaCl	Na_2SO_4
Control	Brick-C-Control	Brick-S-Control	Mortar-C-Control	Mortar-S-Control	B+M-C-Control	B+M-S-Control
TEOS	Brick-C-TEOS	Brick-S-TEOS	Mortar-C-TEOS	Mortar-S-TEOS	B+M-C-TEOS	B+M-S-TEOS

3 Results and Discussions

3.1 Accelerated salt weathering

The mass evolution of specimens during salt weathering typically follows three phases: initial mass gain due to salt crystallisation, a phase of fluctuation, and a final phase of mass loss [10]. In this study, consolidated and unconsolidated specimens were subjected to accelerated weathering by Na_2SO_4 (8 cycles) and NaCl (7 cycles) to assess the effect of consolidation on mass retention. Figure 3 presents the mass variation of the specimens during salt weathering, where the pre-consolidation stage corresponds to partial weathering (initial two cycles of weathering), and the post-consolidation stage represents continued weathering following consolidation treatment. The average of mass variations of two specimens is plotted for each consolidation state within each specimen type. Powdering on the evaporative surface and efflorescence were the main deterioration features, consistent with previous studies [10], [18]. Reduced solution uptake in the final cycles likely resulted from salt accumulation near the suction face, limiting further ingress. The maximum mass increase observed can thus be interpreted as an indicator of salt ingress and storage capacity within the substrate microstructure. TEOS-consolidated specimens exhibited the smallest maximum percentage mass increase during weathering across all specimen types and weathering agents. This behaviour reflects the pore-occluding effect of the amorphous silica gel formed by TEOS and its residual hydrophobicity, which reduces moisture and saline solution uptake [19].

Across all samples, mass increases during the initial two cycles reflect salt uptake and crystallisation within the pore network. Partial pre-weathering induces controlled salt contamination without significant material loss or disintegration. No pronounced differences between brick, mortar, or composite systems are observed at this stage. Following consolidation, chloride-exposed specimens exhibit a general increase in mass up to cycle 6, associated with continued salt ingress and accumulation. TEOS-consolidated bricks show a consistently higher mass gain than controls, indicating enhanced retention of material and salts. Control specimens exhibit a decline after cycle 6, suggesting the onset of material loss. Both TEOS and control mortars display sustained mass gain; however, TEOS-treated mortars maintain slightly higher and more stable mass values across cycles, reflecting improved resistance to chloride-induced degradation. Composite specimens show similar trends for TEOS and controls up to mid-cycles, but TEOS-consolidated systems retain mass more effectively at later cycles, suggesting improved integrity of the assembly under chloride exposure. Overall, chloride weathering leads primarily to salt accumulation rather than severe material loss, with TEOS consolidation enhancing mass stability in all systems.

Sulphate exposure produces markedly different behaviour, characterised by stronger fluctuations and eventual mass loss. Control specimens show a significant mass increase up to 6 cycles, whereas TEOS specimens show a significant mass increase up to 8 cycles, followed by a sharp decrease at later cycles. TEOS-treated bricks retain higher mass than controls, indicating delayed degradation but not complete prevention of sulphate damage. TEOS-consolidated mortars maintain higher mass values throughout most cycles, whereas controls show pronounced oscillations and lower overall mass, reflecting higher susceptibility to sulphate-induced damage. Composite specimens exhibit the most severe response. Both systems gain mass up to cycle 7-8, followed by abrupt mass loss, particularly pronounced in the control. The sharp mass drop of both control and TEOS-consolidated specimens suggests accelerated damage once sulphate crystallisation pressures exceed the material resistance, especially at the brick-mortar interface.

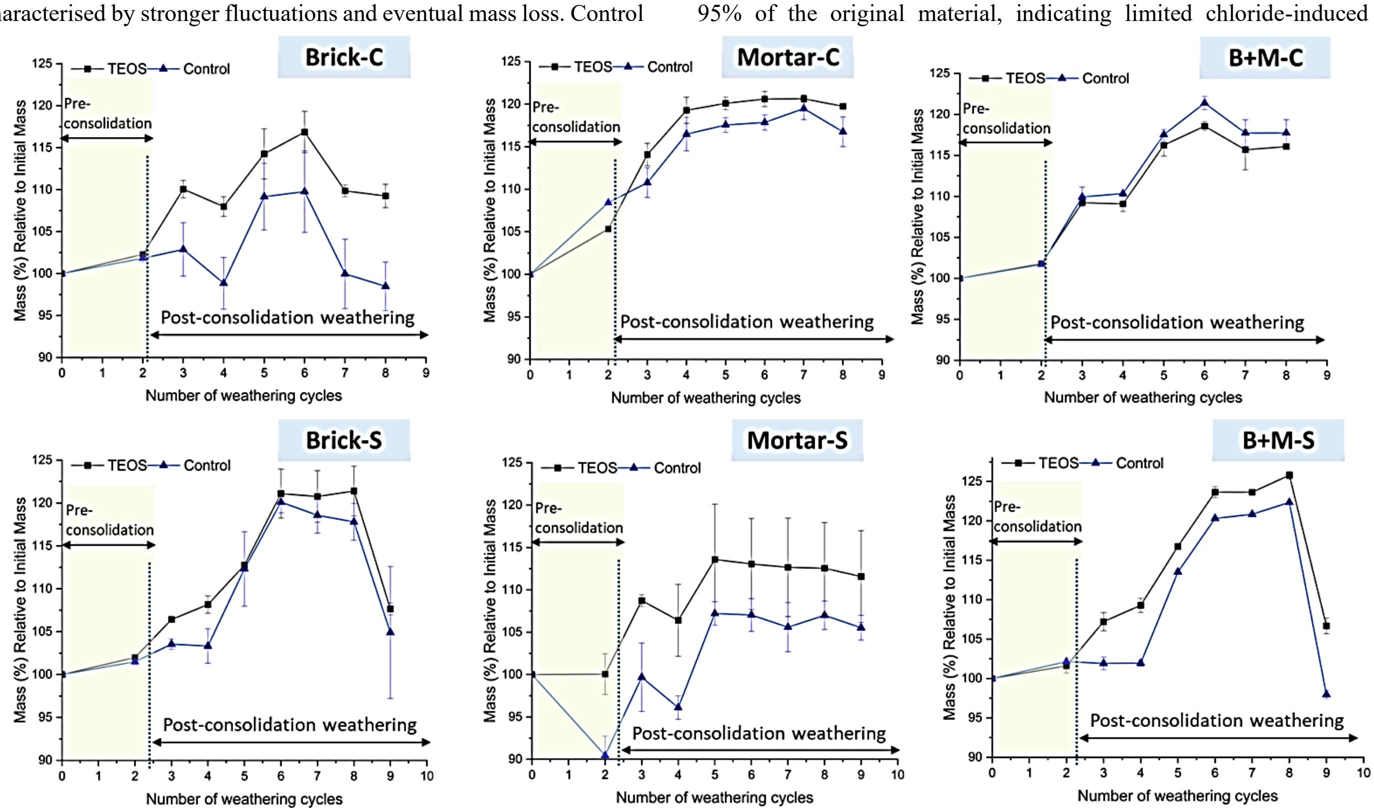

Figure 3 Mass variation during salt weathering

TEOS forms independent silica networks that bond physically with the substrate surface, limiting salt ingress while enhancing mechanical strength. After reaching the maximum mass, specimens lose mass as material degradation outweighs further salt deposition. Consequently, the net residual mass at the end of weathering represents a balance between salt accumulation and material loss, making direct assessment of deterioration challenging [10].

To determine material retention, representative specimens were desalinated in distilled water until solution conductivity stabilised, removing soluble salts and poorly cohesive surface grains, then oven-dried. TEOS-consolidated specimens showed higher retention than unconsolidated controls after both sulphate and chloride weathering (Figure 4), reflecting enhanced mechanical strength and residual hydrophobicity that limit saline ingress. For brick specimens, material retention remains high under both salt exposures. Under chloride weathering, both TEOS-treated and control bricks retain more than 95% of the original material, indicating limited chloride-induced deterioration. Under sulphate weathering, however, a clear distinction emerges: TEOS-consolidated bricks retain nearly all the original material, whereas control specimens show a noticeable reduction. This demonstrates that TEOS consolidation effectively mitigates sulphate-induced material loss in bricks. In the case of mortars, the influence of salt type is more pronounced. Under chloride exposure, both TEOS-treated and control mortars show comparable retention, with only minor differences. In contrast, sulphate weathering causes substantial material loss in unconsolidated mortars, while TEOS-consolidated mortars retain a significantly higher fraction of material. This highlights the greater vulnerability of mortars to sulphate attack and the protective effect of TEOS in limiting surface disintegration. For brick-mortar assemblies (B+M), high material retention is observed under sulphate weathering for both systems, with only marginal differences between TEOS and control specimens. Under chloride exposure, however, TEOS-consolidated assemblies retain a higher proportion of material compared to the controls, indicating delayed degradation. Despite this improvement, the retained material fraction remains lower than that observed for individual brick specimens, reflecting the increased susceptibility of composite systems to salt-induced damage.

Shear tests on sandwich specimens (Figure 5) confirmed improved residual mechanical performance. These findings highlight that effective consolidation of composite substrates depends on (i) mechanical strengthening of individual components via chemical or physical bonding, (ii) pore structure and water transport modifications affecting salt crystallisation, and (iii) the consolidant's influence on interfaces between substrate components.

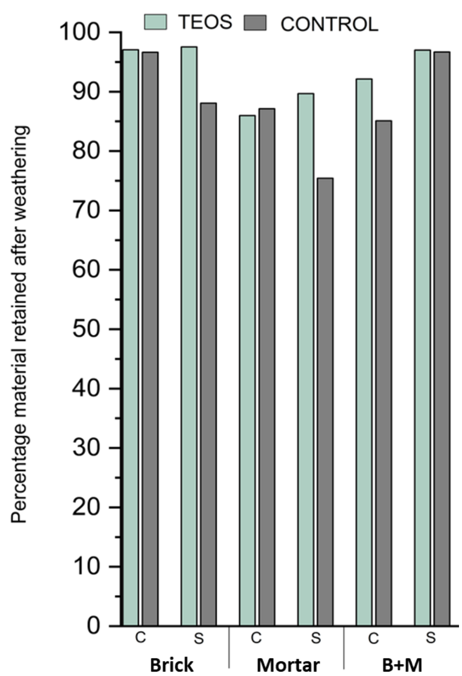

Figure 4 Percentage of material retained after salt weathering

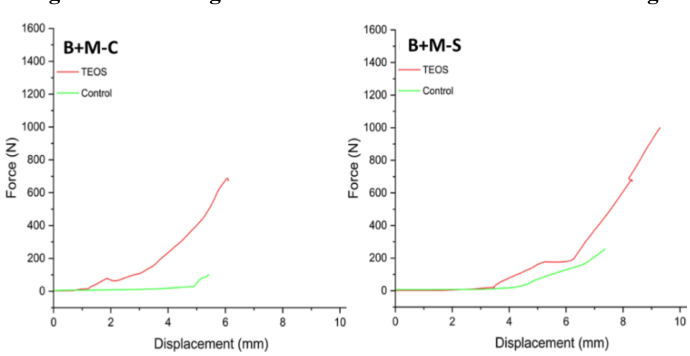

Figure 5 Force-displacement graphs of weathered sandwich specimens during shearing

3.2 Microstructure and mineralogy

Pore size distribution strongly affects moisture transport, salt crystallisation stresses, and salt distribution [20]. In general, the number of larger pores is reduced, and microporosity is increased by consolidation. The susceptibility to damage during salt attack increases with the increase in the number of pores of radius less than 1 µm [21], [22]. Small subsamples were taken from the bottom, middle, and top regions of each specimen for Mercury Intrusion Porosimetry, providing a representative average of the pore structure.

TEOS consolidation refines the pore structure and, upon further weathering, produces a bimodal distribution. TEOS-based treatment is known to cause a significant change in porosity [6], [12]]. In the mortar specimens, salt crystallisation within available pores decreases the larger pore and increases the smaller ones, causing a leftward shift in the pore size distribution (Figure 6). Weathered TEOS-consolidated mortars have a critical pore size of 20-30 nm, whereas that of unconsolidated mortar is around 1000 nm. The critical pore size represents the pore diameter that governs capillary transport and fluid ingress in porous materials. A reduction of the critical pore size by nearly two orders of magnitude following TEOS consolidation substantially restricts the penetration of saline solutions, as smaller pores reduce capillary suction and limit the accessibility of larger, more transport-efficient pathways. As a result, salt entry into the material may be reduced or slowed. However, once salts do penetrate, the crystallisation stress is substantial when the salt crystallises within small pores compared to significantly larger pores, which is attributed to the geometrical differences of crystals in pores of different sizes. Salt crystallisation in an unrestrained, large pore facilitates the attainment of large curvature. In contrast, smaller pores restrain the growth of crystals in some directions and result in lower curvature of crystals in the restrained portions of the pore walls. The latter causes damaging crystallisation pressure that deteriorates the pore walls compared to the former [23]. Hence, the change in pore structure due to TEOS consolidation could adversely affect the material durability with respect to crystallisation in the long term. Additionally, the moisture transport and consequently the distribution of salt depend on the hygroscopicity of the material, which is affected by the change in the pore size distribution [24]. Thus, a reduction in pore size and, thus, the subsequent change in the pore size distribution due to TEOS consolidation could detrimentally affect the long-term durability of materials.

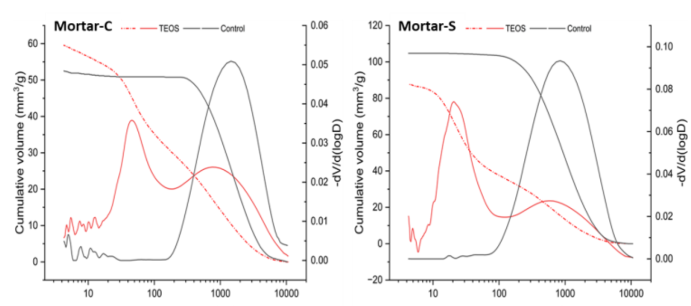

Figure 6 Porosity characteristics of the weathered mortar specimen

Maintaining breathability is essential in masonry, allowing moisture to escape through the sacrificial mortar layer rather than the bricks or stones, which supports long-term durability [8]. Backscattered electron imaging and elemental mapping of sandwich specimens were used to assess salt distribution near the brick–mortar interface. Ten locations were analysed at ~15 µm from the interface in both mortar and brick, and another ten at ~100 µm away, enabling quantification of salt content at and away from the interface. Figure 7 shows salt distribution at the interfaces of B+M-C and B+M-S sandwich specimens, comparing TEOS-consolidated and unconsolidated controls. Colour maps indicate salt concentration, with red representing the highest and green the lowest, with gradients reflecting specimen-specific ranges. Salt transport during drying highlights moisture pathways critical for durability. Accumulation in the mortar (red regions) rather than the brick confirms maintained breathability, directing deterioration to the mortar, a preferred outcome, as damage to bricks or stones compromises structural stability and is harder to repair.

For B+M-C-Control, near the interface, high salt concentrations are observed on both the brick (-15 µm) and mortar (+15 µm) sides, with particularly elevated values in the mortar. Away from the interface, significant salt contents persist in both the brick (-100 µm) and mortar (+100 µm), indicating unrestricted chloride transport across the assembly. This behaviour reflects the open pore network of the unconsolidated system and explains the high susceptibility to interfacial and bulk salt damage. Compared to the control, TEOS consolidation reduces salt accumulation away from the interface, especially within the brick (-100 mm). However, pronounced salt concentrations remain close to the interface, particularly within the mortar (+15 mm), suggesting that pore refinement limits long-range transport but promotes localised salt accumulation near hygric discontinuities. This indicates partial salt trapping at the interface despite reduced overall chloride ingress.

Sulphate-contaminated control specimens show relatively uniform salt distributions across both brick and mortar, with moderate accumulation near the interface and sustained presence away from it. This reflects repeated sulphate dissolution-recrystallisation throughout the system and supports the occurrence of distributed microstructural damage rather than purely interfacial deterioration. TEOS consolidation significantly reduces sulphate penetration into the bulk brick (-100 mm) and mortar (+100 mm). Nevertheless, localised salt enrichment is observed near the interface, particularly on the mortar side (+15 mm). Given the refined pore structure induced by TEOS, sulphate crystallisation in this near-interface zone is likely to generate high crystallisation pressures, promoting microfissuring and contributing to the reduced shear strength observed in the consolidated sandwich specimens.

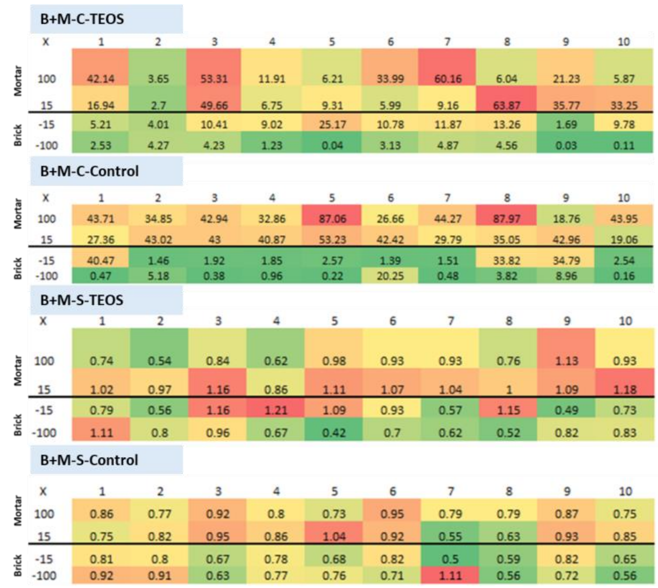

B+M-C-TEOS

	X	1	2	3	4	5	6	7	8	9	10
Mortar	100	42.14	3.65	53.31	11.91	6.21	33.99	60.16	6.04	21.23	5.87
Mortar	15	16.94	2.7	49.66	6.75	9.31	5.99	9.16	63.87	35.77	33.25
Brick	-15	5.21	4.01	10.41	9.02	25.17	10.78	11.87	13.26	1.69	9.78
Brick	-100	2.53	4.27	4.23	1.23	0.04	3.13	4.87	4.56	0.03	0.11

B+M-C-Control

	X	1	2	3	4	5	6	7	8	9	10
Mortar	100	43.71	34.85	42.94	32.86	87.06	26.66	44.27	87.97	18.76	43.95
Mortar	15	27.36	43.02	43	40.87	53.23	42.42	29.79	35.05	42.96	19.06
Brick	-15	40.47	1.46	1.92	1.85	2.57	1.39	1.51	33.82	34.79	2.54
Brick	-100	0.47	5.18	0.38	0.96	0.22	20.25	0.48	3.82	8.96	0.16

B+M-S-TEOS

	X	1	2	3	4	5	6	7	8	9	10
Mortar	100	0.74	0.54	0.84	0.62	0.98	0.93	0.93	0.76	1.13	0.93
Mortar	15	1.02	0.97	1.16	0.86	1.11	1.07	1.04	1	1.09	1.18
Brick	-15	0.79	0.56	1.16	1.21	1.09	0.93	0.57	1.15	0.49	0.73
Brick	-100	1.11	0.8	0.96	0.67	0.42	0.7	0.62	0.52	0.82	0.83

B+M-S-Control

	X	1	2	3	4	5	6	7	8	9	10
Mortar	100	0.86	0.77	0.92	0.8	0.73	0.95	0.79	0.79	0.87	0.75
Mortar	15	0.75	0.82	0.95	0.86	1.04	0.92	0.55	0.63	0.93	0.85
Brick	-15	0.81	0.8	0.67	0.78	0.68	0.82	0.5	0.59	0.82	0.65
Brick	-100	0.92	0.91	0.63	0.77	0.76	0.71	1.11	0.56	0.72	0.56

Figure 7 Salt distribution near and away from the interface of the sandwich samples

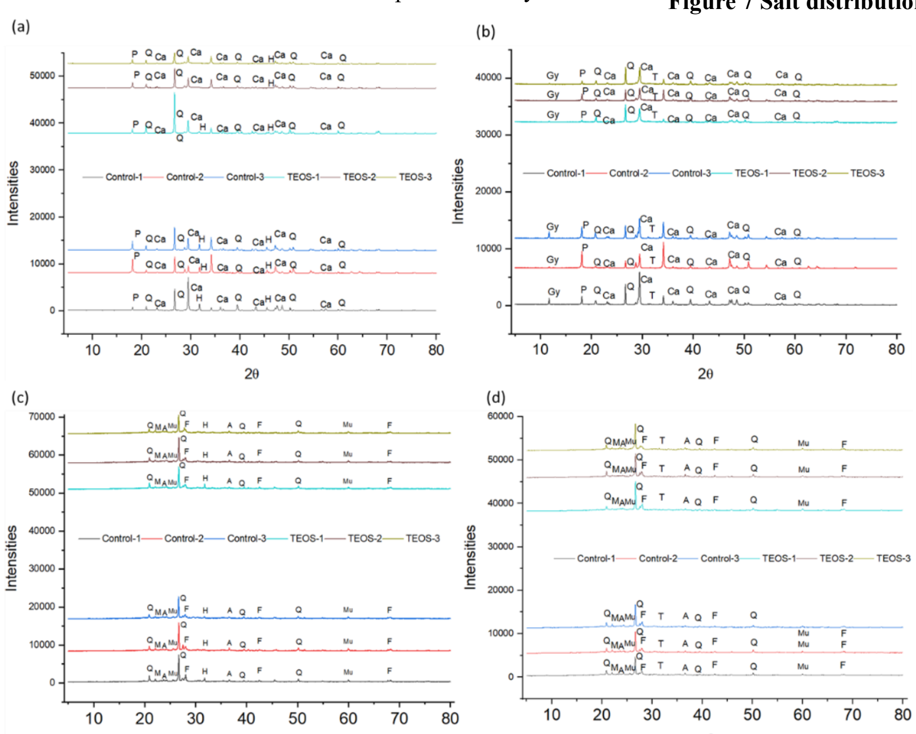

Figure 8 Diffractograms of mortar samples after (a) chloride weathering and (b) sulphate weathering, and brick samples after (c) chloride weathering and (d) sulphate weathering (Q: Quartz, Ca: Calcite, P: Portlandite, H: Halite, Gy: Gypsum, T: Thenardite, F: Feldspar, A: Albite, M: Magnetite)

Table 2 Halite and sulphate (thenardite (T) + gypsum (G)) percentages in the samples quantified through X-Ray diffraction

Specimens	Salt	Average percentage of salt in specimens (%)	Specimens	Type of salt	Average percentage of salt in specimens (%)	
Brick-C-Control	Chloride	11.42	Brick-S-Control	Sulphate	8.45	(T: 8.45, G: 0)
Brick-C-TEOS	Chloride	0.54	Brick-S-TEOS	Sulphate	7.38	(T: 7.38, G: 0)
Mortar-C-Control	Chloride	4.84	Mortar-S-Control	Sulphate	4.21	(T: 1.17, G: 3.04)
Mortar-C-TEOS	Chloride	1.21	Mortar-S-TEOS	Sulphate	1.50	(T: 1, G: 0.5)

Figure 7 shows that breathability is preserved in all consolidation states, with lower chloride concentrations in bricks (green) and higher in mortars (yellow-red). Unconsolidated specimens exhibit severe chloride accumulation near the interface. A moderate concentration of chloride ions was depicted on the mortar phase of the TEOS-consolidated specimen with isolated peaks of higher concentration near the interface. Hence, the resistance offered by the TEOS treatment to chloride ingress can be considered moderate. The illustration indicates severe salt ingress and accumulation and an elevated salt concentration at the interface, though it reduces as the distance from the interface increases. Interfaces consistently exhibit the highest salt concentrations, highlighting their key role in transport.

Figure 7 shows lower sulphate concentrations than chloride ion concentrations due to larger ion size and lower mobility, with localised interface accumulations confirming its critical role. Brick phases remain largely unaffected, maintaining overall breathability.

Figure 8 shows the diffractograms of weathered samples, and Table 2 shows the percentage of halite and sulphate in the samples quantified through X-ray diffraction. Gypsum was found in the mortar specimens due to residual portlandite reacting with sulphate ions:

$Ca(OH)_2 + Na_2SO_4 + 2H_2O \rightarrow CaSO_4 \cdot 2H_2O + 2NaOH$.

Gypsum precipitation, facilitated by wetting–drying cycles, generates crystallisation stresses, particularly in smaller pores, promoting microcracks and material loss. Gypsum crystallisation in larger pores can block transport pathways, exacerbating stress. Quantitative XRD (Table 2) shows that TEOS consolidation effectively limits salt ingress across all specimens and salt types, reducing both chloride and sulphate accumulation.

4 Conclusions

The study assessed mass changes, microstructural alterations, crystallisation products formation and mineralogical changes in bricks, mortars and their composite systems exposed to sodium chloride and sodium sulphate weathering following consolidation with TEOS. The observations on individual components and masonry sandwiches allowed to derive the following conclusions:

- TEOS consolidation induces pronounced pore refinement through partial pore filling by silica gel, with Mercury Intrusion Porosimetry indicating a reduction of the critical pore size from the micrometre scale (~1000 nm in unconsolidated mortars) to the nanometre scale (20 - 30 nm). This refinement, together with residual hydrophobic effects despite accelerated curing, limits salt ingress into TEOS-treated substrates.
- As a consequence, TEOS-treated specimens show enhanced material retention under both chloride and sulphate weathering, in individual materials as well as in composite brick–mortar systems. This confirms the effectiveness of TEOS in improving near-surface cohesion and resistance to salt-induced material loss.
- Chloride exposure primarily leads to progressive salt accumulation with limited mechanical damage, and TEOS consolidation enhances mass stability across all tested systems. In contrast, sulphate weathering induces cyclic damage associated with crystallisation pressure, phase transformations, and volumetric expansion. Although TEOS delays deterioration, it does not fully prevent sulphate-induced damage at advanced cycles, particularly in composite systems, highlighting the strong interaction between sulphate salts and pore-refined materials.
- Mechanical testing corroborates the mass retention trends, showing that TEOS consolidation increases shear failure loads in brick–mortar assemblies. However, the improved mechanical performance must be interpreted alongside the observed microstructural changes, as excessive pore refinement may increase crystallisation stresses under aggressive salt exposure.
- Breathability was not directly quantified; however, BSE imaging combined with elemental point analysis indicates that TEOS consolidation alters, rather than completely blocks, moisture and salt transport pathways. The preferential localisation of salts near the brick–mortar interface suggests that TEOS limits long-range transport while potentially promoting localised salt accumulation, underscoring the delicate balance between beneficial pore refinement and detrimental pore occlusion.
- The formation of gypsum after sulphate weathering was attributed to the reaction between sulphate ions and residual portlandite in the mortar, despite prior natural carbonation. Gypsum formation contributed to additional mortar deterioration and reinforced the vulnerability of lime-based mortars under sulphate-rich conditions.

Overall, the results indicate that TEOS may improve the short-term resistance of masonry materials to salt weathering; however, its pore-refining effects introduce potential risks that require careful consideration in conservation practice. The study highlights the narrow operational margin between improved cohesion and increased salt-related risks, emphasizing the need for consolidation strategies that balance mechanical improvement with pore-scale compatibility. These findings contribute to a more performance-based understanding of consolidation treatments for masonry exposed to saline environments.

Acknowledgements

The authors would like to gratefully acknowledge the funding from the Ministry of Education, Government of India, towards the Fellowship of the first author. The authors are grateful to the Building Technology and Construction Management (BTCM) Division, Department of Civil Engineering at the Indian Institute of Technology Madras, India, and DICAM laboratory at the University of Bologna, Italy, for providing the laboratory facilities.

Statements and Declarations

The authors report no potential conflict of interest.

Data availability statement

Any additional data or specific requests for data that are not publicly available can be obtained from the corresponding author upon reasonable request.

References

[1]. A. Menon, "Heritage Conservation in India: Challenges and New Paradigms," SAHC2014 – 9th Int. Conf. Struct. Anal. Hist. Constr., no. October, pp. 14–17, 2014.

[2]. V. A. Anupama and M. Santhanam, "Salt weathering resilience in masonry: An accelerated laboratory study involving wind-induced variations," Constr. Build. Mater., vol. 449, p. 138360, Oct. 2024, doi: 10.1016/j.conbuildmat.2024.138360.

[3]. R. J. Flatt, "Salt damage in porous materials : how high supersaturations are generated," J. Cryst. Growth, vol. 242, pp. 435–454, 2002.

[4]. J. He et al., "Ethyl silicate–nanolime treatment for the consolidation of calcareous building materials," Constr. Build. Mater., vol. 418, no. November 2023, 2024, doi: 10.1016/j.conbuildmat.2024.135437.

[5]. G. Masi, A. Dal Pozzo, G. Ugolotti, A. Tugnoli, and E. Sassoni, "Choosing the consolidant for carbonate substrates: Technical performance and environmental sustainability of selected inorganic and organic products," Constr. Build. Mater., vol. 407, no. May, 2023, doi: 10.1016/j.conbuildmat.2023.133599.

[6]. E. Sassoni, E. Franzoni, B. Pigino, G. W. Scherer, and S. Naidu, "Consolidation of calcareous and siliceous sandstones by hydroxyapatite: Comparison with a TEOS-based consolidant," J. Cult. Herit., vol. 14, no. 3 SUPPL, pp. e103–e108, 2013, doi: 10.1016/j.culher.2012.11.029.

[7]. A. P. Ferreira Pinto and J. Delgado Rodrigues, "Consolidation of carbonate stones: Influence of treatment procedures on the strengthening action of consolidants," J. Cult. Herit., vol. 13, no. 2, pp. 154–166, 2012, doi: 10.1016/j.culher.2011.07.003.

[8]. G. Masi and E. Sassoni, "Air lime mortar consolidation by nanolimes and ammonium phosphate: Compatibility, effectiveness and durability," Constr. Build. Mater., vol. 299, p. 123999, Sep. 2021, doi: 10.1016/j.conbuildmat.2021.123999.

[9]. V. A. Anupama, E. Sassoni, and M. Santhanam, "Consolidants in Salt-Weathered Masonry: Retention and Efficiency of DAP and TEOS," RILEM Tech. Lett., vol. 9, pp. 76–86, Jan. 2025, doi: 10.21809/rilemtechlett.2024.206.

[10]. E. Sassoni, G. Graziani, and E. Franzoni, "An innovative phosphate-based consolidant for limestone. Part 2: Durability in comparison with ethyl silicate," Constr. Build. Mater., vol. 102, pp. 931–942, 2016, doi: 10.1016/j.conbuildmat.2015.10.202.

[11]. G. W. Scherer and G. S. Wheeler, "Silicate consolidants for stone," Key Eng. Mater., vol. 391, pp. 1–25, 2009, doi: 10.4028/www.scientific.net/kem.391.1.

[12]. P. Martinez, M. Soto, F. Zunino, C. Stuckrath, and M. Lopez, "Effectiveness of tetra-ethyl-ortho-silicate (TEOS) consolidation of fired-clay bricks manufactured with different calcination temperatures," Constr. Build. Mater., vol. 106, pp. 209–217, 2016, doi: 10.1016/j.conbuildmat.2015.12.116.

[13]. T. D. Singh, S. Prakash, and S. Manohar, "Assessment of the performance and compatibility of acrylic polymer and silane based consolidants on deteriorated heritage masonry units subjected to salt weathering," J. Build. Eng., vol. 77, no. June, p. 107490, 2023, doi: 10.1016/j.jobe.2023.107490.

[14]. E. Franzoni, G. Graziani, and E. Sassoni, "TEOS-based treatments for stone consolidation: acceleration of hydrolysis–condensation reactions by poulticing," J. Sol-Gel Sci. Technol., vol. 74, no. 2, pp. 398–405, 2015, doi: 10.1007/s10971-014-3610-3.

[15]. [A. M. Barberena-Fernández, P. M. Carmona-Quiroga, and M. T. Blanco-Varela, "Interaction of TEOS with cementitious materials: Chemical and physical effects," Cem. Concr. Compos., vol. 55, pp. 145–152, 2015, doi: 10.1016/j.cemconcomp.2014.09.010.

[16]. A. M. Barberena-Fernández, M. T. Blanco-Varela, and P. M. Carmona-Quiroga, "Use of nanosilica- or nanolime-additioned TEOS to consolidate cementitious materials in heritage structures: Physical and mechanical properties of mortars," Cem. Concr. Compos., vol. 95, no. August 2018, pp. 271–276, 2019, doi: 10.1016/j.cemconcomp.2018.09.011.

[17]. Barbara. Lubelli et al., "Recommendation of RILEM TC 271-ASC: New accelerated test procedure for the assessment of resistance of natural stone and fired-clay brick units against salt crystallization," Mater. Struct. Constr., vol. 56, no. 5, 2023, doi: 10.1617/s11527-023-02158-0.

[18]. B. Lubelli, R. P. J. van Hees, and T. G. Nijland, "Salt crystallization damage: how realistic are existing ageing tests?," Proc. Int. Conf. Ageing Mater. Struct., vol. 2, no. 1, pp. 103–111, 2014.

[19]. G. M. C. Gemelli, R. Zarzuela, F. Fernandez, and M. J. Mosquera, "Compatibility, effectiveness and susceptibility to degradation of alkoxysilane-based consolidation treatments on a carbonate stone," J. Build. Eng., vol. 42, no. June, p. 102840, 2021, doi: 10.1016/j.jobe.2021.102840.

[20]. B. Sena da Fonseca, A. P. Ferreira Pinto, M. Rucha, M. M. Alves, and M. F. Montemor, "Damaging effects of salt crystallizationn a porous limestone after consolidation treatments," Constr. Build. Mater., vol. 374, no. March, p. 130967, 2023, doi: 10.1016/j.conbuildmat.2023.130967.

[21]. G. Graziani, E. Sassoni, and E. Franzoni, "Consolidation of porous carbonate stones by an innovative phosphate treatment: Mechanical strengthening and physical-microstructural compatibility in comparison with TEOS-based treatments," Herit. Sci., vol. 3, no. 1, 2015, doi: 10.1186/s40494-014-0031-0.

[22]. A. Murru and R. Fort, "Diammonium hydrogen phosphate (DAP) as a consolidant in carbonate stones: Impact of application methods on effectiveness," J. Cult. Herit., vol. 42, pp. 45–55, 2020, doi: 10.1016/j.culher.2019.09.003.

[23]. S. Manohar, "A study on characterisation, deterioration mechanisms and protection of bricks and stones in historic structures," 2020.

[24]. [24] A. E. Charola, "Salts in the deterioration of porous materials: An overview," J. Am. Inst. Conserv., vol. 39, no. 3, pp. 327–343, 2000, doi: 10.1179/019713600806113176.